

See discussions, stats, and author profiles for this publication at: <https://www.researchgate.net/publication/231665417>

# SAFT–VRE: Phase Behavior of Electrolyte Solutions with the Statistical Associating Fluid Theory for Potentials of Variable Range

ARTICLE *in* THE JOURNAL OF PHYSICAL CHEMISTRY B · NOVEMBER 1999

Impact Factor: 3.3 · DOI: 10.1021/jp991959f

CITATIONS

125

READS

89

## 4 AUTHORS, INCLUDING:



[Amparo Galindo](#)

Imperial College London

117 PUBLICATIONS 3,851 CITATIONS

SEE PROFILE



[Alejandro gil-villegas](#)

Universidad de Guanajuato

78 PUBLICATIONS 2,010 CITATIONS

SEE PROFILE



[Andrew N. Burgess](#)

AkzoNobel

59 PUBLICATIONS 1,892 CITATIONS

SEE PROFILE

# SAFT-VRE: Phase Behavior of Electrolyte Solutions with the Statistical Associating Fluid Theory for Potentials of Variable Range

Amparo Galindo,<sup>†</sup> Alejandro Gil-Villegas,<sup>‡</sup> George Jackson,<sup>\*,†</sup> and Andrew N. Burgess<sup>§</sup>

Department of Chemical Engineering and Chemical Technology, Imperial College of Science, Technology and Medicine, Prince Consort Road, London SW7 2Y, U.K., Instituto de Física, Universidad de Guanajuato, León 37150, México, and Research and Technology, ICI Chemicals and Polymers, PO Box 8, The Heath, Runcorn, Cheshire WA7 4QD, U.K.

Received: June 14, 1999; In Final Form: August 26, 1999

A modification of the statistical associating fluid theory has recently been developed to model non-conformal fluids with attractive potentials of variable range (SAFT-VR) [Gil-Villegas, A.; Galindo, A.; Whitehead, P. J.; Mills, S. J.; Jackson, G.; Burgess, A. N. *J. Chem. Phys.* **1997**, *106*, 4168] which gives a very good description of the phase behaviour of water and its mixtures with nonelectrolytes. In the present paper we extend the SAFT-VR approach to deal with strong-electrolyte solutions (SAFT-VRE). The water molecules are modeled as hard spheres with four attractive short-range sites to describe the hydrogen-bonding association. The electrolyte molecules are modeled with two hard spheres of different size which describe the anion and cation respectively. The mean-spherical approximation (MSA) is used for the restricted primitive model (RPM) to account for the long-range Coulombic ion–ion interactions, while the long-range water–water and ion–water attractive interactions are modeled as square-well dispersive interactions treated via a second-order high-temperature expansion in the spirit of the SAFT-VR approach. We have studied nine single-salt aqueous solutions and one mixed-salt system of characteristic strong electrolytes (alkali halides) in the temperature range between 273 and 373 K. Using only one transferable fitted parameter per ion, the experimental vapor pressures and densities are very well described by the SAFT-VRE theory. As a limit of the MSA, the Debye–Hückel (DH) expression is used to describe the ion–ion interactions in one of the solutions. Due to the excellent description of the solvent in the SAFT-VR approach, the experimental vapor pressure for an aqueous solution of sodium chloride is also very well described with this simple approach.

## 1. Introduction

When an inorganic salt is dissolved in water it dissociates into positive and negative ions (cations and anions) forming an electrolyte solution. Different solutes dissociate to different extent; electrolytes are often classified as weak and strong according to the degree of dissociation. In strong electrolytes the solute is believed to exist only in the form of simple cations and anions (possibly solvated); the most common example of a strong electrolyte is aqueous sodium chloride (NaCl). In general the aqueous solutions of alkali halides, and the alkaline-earth halides and perchlorates, are also considered to be fully dissociated electrolytes. In weak electrolytes the molecular species coexists in equilibrium with the free ions. Robinson and Stokes<sup>1</sup> described these as “associated” solutions (strong electrolyte solutions being “nonassociated”) and noted the difference between “weak electrolytes”, in which it is the covalent species that remain present in equilibrium with the free ions (all acids and most bases belong to this class), and “ion-pairing electrolytes”, in which association occurs due to the electrostatic attraction between positive and negative ions only; a concept first introduced by Bjerrum.<sup>2</sup> Bivalent metal sulphates in aqueous solutions and almost all other salts in nonaqueous solvents show evidence of such pairing. A rigid classification into strong and weak electrolytes (or nonassociated and associ-

ated), however, applies only to ambient temperatures and pressures. It has been shown that ion pairing occurs in all aqueous electrolyte solutions as the temperature approaches the critical point of water due to the decrease in the dielectric constant of water.<sup>3,4</sup> The temperature at which ion pairing first becomes important also depends on the solute, but in general it tends to be lower when the ionic charges are higher. The distinction between strong and weak electrolytes usually holds for temperatures up to 523 K and sometimes higher. For example, Palaban and Pitzer measured the heat capacity of KCl solutions and no change was recorded even at 599 K.<sup>5</sup> A detailed description of ion-association mechanisms in near-critical and supercritical aqueous solutions of NaCl have been studied recently with molecular dynamics by Cummings and co-workers.<sup>4,6</sup>

The complex nature of the electrolyte solutions has attracted the attention of the scientific community for more than a century: the solutions find direct application in the chemical industry (desalination plants, humidity control systems, air conditioning, etc.), in geochemical systems (hydrothermal activity, hot springs, ore deposits, etc.), and are fundamental to biological activity (Na<sup>+</sup>–K<sup>+</sup> equilibrium, etc.). Extensive and reliable experimental data of thermophysical properties of aqueous electrolyte solutions are readily available, especially at ambient conditions,<sup>7,8</sup> although experimental difficulties mean that considerably less data has been obtained at high temperatures and pressures.<sup>9,10</sup> Similarly, the quest for theoretical

<sup>†</sup> Imperial College of Science, Technology and Medicine.

<sup>‡</sup> Universidad de Guanajuato.

<sup>§</sup> ICI Chemicals and Polymers.

models aimed at understanding the marked nonideality of such solutions date as far back as the initial experimental efforts.

The first theoretical model is probably that of Arrhenius,<sup>11</sup> who proposed the dissociation of the salts in the solvent. The most influential contribution, however, must be that of Debye and Hückel. In the Debye–Hückel (DH) approach the solution is represented with the ions as point charges in a uniform dielectric medium;<sup>12–14</sup> with this model the electrostatic potential energy between the ions can be obtained by solving a linearized Poisson–Boltzmann equation. The DH solution is exact in the limit of infinite dilution, but at higher concentrations (molality  $m > 0.001$ ), as the size of the ions becomes important, the theory no longer provides an accurate description of the system. It can be extended to take into account ion sizes<sup>15</sup> in order to give reasonable results up to  $m = 0.1$ , and higher order terms in the solution of the Poisson–Boltzmann equation can also be considered; a combination of the DH term with these higher order terms and a reduced number of empirical parameters gives a very accurate representation of the thermodynamic properties of electrolyte solutions as has been shown by Pitzer.<sup>16–18</sup>

More recently, integral equations have been applied to electrolyte solutions. The ion sizes are taken into account in these approaches, and detailed structural information as well as the thermodynamic properties are obtained.<sup>13,15</sup> The mean spherical approximation (MSA) is especially suited to electrolyte solutions as it provides reasonably accurate analytical solutions for primitive models (the solvent is assumed to be uniform and is treated through a dielectric constant). Waisman and Lebowitz<sup>19</sup> presented an analytical solution within the MSA for a system of charged hard spheres of equal finite size (restricted primitive model (RPM)). Blum<sup>20</sup> later extended the MSA description to the general case of spheres of different sizes using the method of Baxter.<sup>21</sup> Adelman and Deutch<sup>22</sup> presented an exact solution for a mixture of equal radii hard spheres with permanent dipole moments. They showed that the mixture can be reduced to a two-component fluid with one charged species and one dipolar species providing a treatment of ionic solutions with a molecular solvent. In general, the MSA models have found widespread use, especially the RPM whose solution is of comparable simplicity to the DH approach.

Loeche and Donohue<sup>23</sup> have recently published an excellent review on the available theoretical models for the description of the thermodynamic properties of strong electrolytes, from fundamental theories such as the MSA to the empirical models used in engineering problems. In the present discussion we concentrate on some of the approaches more closely related to our own (for a more detailed account of models for strong aqueous electrolytes the reader should consult ref 23). Shiah and Tseng<sup>24</sup> have correlated the vapor pressures of 26 aqueous electrolytes using three adjustable parameters. They use the extended MSA description for ions of different sizes: the cation is considered to be solvated and so its diameter is assumed to vary with the salt concentration, while the anion is assumed to be nonhydrated and to have a fixed diameter.<sup>25</sup> Planche and Renon<sup>26</sup> have developed a simplified expression for the MSA screening parameter in a model where the molecules are considered as hard spheres of different sizes with short-range repulsive interactions, and have calculated the osmotic coefficients for a number of strong electrolytes up to  $6m$ . A similar idea has been followed by Copeman and Stein<sup>27</sup> who have incorporated an electrostatic contribution based on the MSA into an equation of state for hard-sphere mixtures which has a perturbation term for the attractive contribution. They have correlated the mean ionic activity coefficients for 13 strong 1:1,

1:2, and 2:1 electrolytes using the Pauling and estimated Bondi diameters for the ions, although the main purpose of their study was to model the water–aniline liquid–liquid equilibrium in the presence of a salt. The size parameters for the solvents were determined from vapor pressure and liquid density data and good agreement was obtained for the distribution coefficients of NaBr and  $\text{NH}_4\text{Cl}$  at 323.15 K.

Perturbation theories have also been applied to electrolyte solutions; in general, the Hemholtz free energy is expanded as an inverse-temperature series, providing a simple route to other thermodynamic properties through differentiation and integration. Stell and Lebowitz<sup>28</sup> developed a perturbation approach for the primitive model, while Henderson et al.<sup>29</sup> solved the expansion for the ion–dipole model. Chan<sup>30,31</sup> has applied the perturbation theory to real aqueous electrolyte solutions in two more recent articles. In the first paper,<sup>30</sup> the perturbation theory of Stell and Lebowitz for the RPM was used to describe the ion–ion interactions, while the Carnahan and Starling hard-sphere equation<sup>32</sup> was used for the repulsive contribution.<sup>30</sup> The ion diameters were fitted to experimental activity coefficients. Although good agreement was obtained for the activities, Chan noted that the values of the resulting diameters did not follow the trends shown by the Pauling experimental diameter data. Chan also commented on the importance of the repulsive term and tested an equation in which the six-term expansion of Stell and Lebowitz was substituted by the simpler DH equation. Little difference is found between the two approaches, which indicates that the main improvement over the DH approximation comes from the hard-sphere properties. In the second paper<sup>31</sup> the ion–dipole perturbation expansion of Henderson et al.<sup>29</sup> was used. Although better agreement was expected since the solvent was treated more realistically, in this case the opposite was observed. The cause of the greater disagreement for the dipole–ion model may lay in the fact that of the three terms in the perturbation expansion of Henderson et al., which account for ion–ion, ion–dipole, and dipole–dipole interactions, Chan only took the leading ion–ion term. Following a slightly different approach Jin and Donohue<sup>33–35</sup> have extended the ideas of the perturbed anisotropic chain theory (PACT) to study electrolyte systems. Using a perturbation expansion of the different interaction potentials they treated molecule–molecule interactions, charge–charge interactions, and charge–molecule interactions. A primitive model was used in which the dielectric constant corrects for the solvation effect, but additional terms are also added to the perturbation expansion to account for interactions between ions and molecules in the bulk solution. Very good agreement was obtained using one size-dependent adjustable parameter for an extensive number of electrolyte systems, including solutions of multiple salts.

In this paper we focus on extending the applicability of the statistical associating fluid theory (SAFT) to electrolyte solutions. The SAFT approach stems from the thermodynamic perturbation theory of Wertheim for associating fluids.<sup>36–39</sup> In its original formulation associating chains of Lennard-Jones segments were considered,<sup>40,41</sup> and the SAFT equation of state was used very successfully to correlate the phase behavior of a large number of pure components and mixtures of complex fluids.<sup>42,43</sup> A simpler version of the SAFT approach (SAFT-HS) in which the dispersion forces are treated at the mean-field level of van der Waals has also been used to predict the phase behavior of a wide range of fluids, and transferable parameters can be obtained which allow one to study an entire series of homologous components with very little experimental information.<sup>44–46</sup> More recently the SAFT equation has been

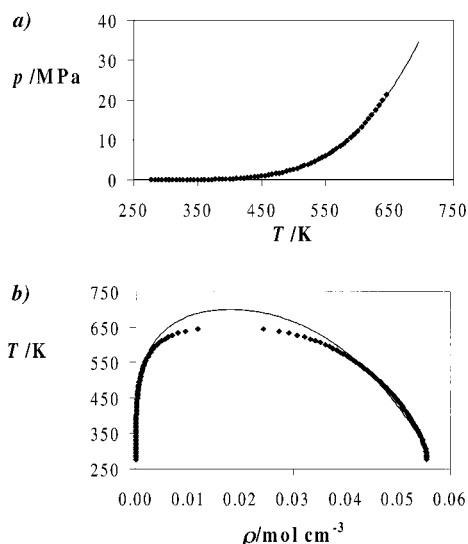


**Figure 1.** (a) Experimental vapor pressures and (b) gas-liquid coexistence densities for water compared with the SAFT-VR predictions (see text for details). The symbols correspond to the experimental data and the solid curves to the calculations.

extended to fluids of associating chain molecules with attractive potentials of variable range (SAFT-VR).<sup>47,48</sup> In this approach the contribution to the free energy due to the dispersion forces is obtained via a second-order high-temperature expansion of the variable-range potential, typically a square well. The extra non-conformal parameter characterising the potential range greatly enhances the performance of the equation in theoretical as well as applied predictions.<sup>49–53</sup> The SAFT approach is especially suited to associated fluids such as water; excellent agreement has been obtained for the vapor pressures and saturated liquid densities<sup>54</sup> (see Figure 1). A good description of water is essential as the first step in obtaining a model of aqueous electrolyte solutions. As the first extension of the SAFT-VR approach to model aqueous electrolyte solutions, the ion–ion interactions are included at the simplest restricted primitive level in this paper. We use experimental data whenever possible to determine the parameters for the ions in the salt. We examine the depletion in the vapor pressure with added salt, and the densities of the solutions, as predicted by the theory, making comparisons with the experimental data for a number of salts in water.

## 2. Models and Theory

We use the same general model for water as presented in previous work, which has been shown to give a very good description of the vapor pressure and coexistence densities of water and its mixtures.<sup>44–46,54</sup> The water molecules are modeled as hard spheres of diameter  $\sigma_{11}$  with four short-ranged off-center attractive square-well sites which mediate association (Figure 2a). Two of the sites represent the hydrogens in the molecule and the other two the oxygen lone pairs. The sites are situated off-center at a distance  $r_{d1}$ , and when two sites are closer than a distance  $r_{c1}$  they interact with an attractive energy  $\epsilon_{11}^{\text{HB}}$ . Although the relative positions of the sites are not important at this level of approximation, they can be viewed as being situated in a tetrahedral arrangement on the sphere. In the SAFT-VR approach the weak long-range attractive forces are modeled via a second-order high-temperature expansion; we use a square-well potential of range  $\lambda_{11}$  and depth  $\epsilon_{11}$  for the water molecules. The SAFT-VR description of this model provides vapor pressures and coexistence densities which are in excellent

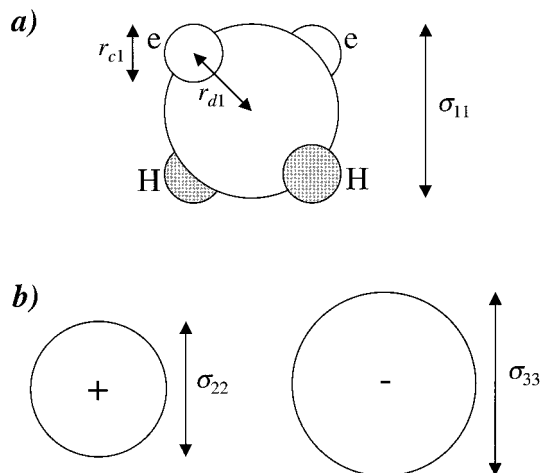


**Figure 2.** Models for (a) water molecule and (b) cation and anion. The water molecule is modeled with four off-center square-well sites placed on a sphere of diameter  $\sigma_{11}$ . The sites are at a distance  $r_{d1}$  from the center of the sphere. Two of the sites represent the hydrogen atoms (H) and the other two the oxygen lone pairs of electrons (e). An H–e hydrogen-bond interaction of attractive energy  $\epsilon_{11}^{\text{HB}}$  occurs when two sites are closer than  $r_{c1}$ . Long-range dispersion interactions are modeled via a second-order high-temperature expansion for a square-well potential of range  $\lambda_{11}$  and depth  $\epsilon_{11}$ . Two hard spheres of diameters  $\sigma_{22}$  and  $\sigma_{33}$  model the cation and anion respectively in what concerns the repulsive interactions. Ion–ion interactions are modeled with the mean spherical approximation using an average diameter and the experimental dielectric constant of the solvent (see text).

agreement with the experimental data.<sup>54</sup> The salt molecules are modeled with two hard spheres of diameters  $\sigma_{22}$  and  $\sigma_{33}$  which represent the cation and anion, respectively. Planche and Renon,<sup>26</sup> and later Chan,<sup>30</sup> have shown that simple models for the Coulombic interaction are very much improved by including the hard-sphere repulsions of the fluid. Following this spirit, we model the ion–ion Coulombic interactions in a very simple way using the MSA solution of the RPM. An equal average diameter is used for the two ions which are assumed to be in a uniform dielectric medium. Water–ion long-range attractive interactions are taken into account with the SAFT-VR second-order high-temperature expansion for square-well potentials of ranges  $\lambda_{12}$  and  $\lambda_{13}$  and depths  $\epsilon_{12}$  and  $\epsilon_{13}$ . One should note that ion–ion interactions occur exclusively through the Coulombic contribution, which we describe with the MSA in the RPM including a dielectric constant which takes care of the effective ion–ion electrostatic interaction due to the presence of the solvent; square-well ion–ion interactions are thus not included ( $\epsilon_{22} = 0$ ,  $\epsilon_{33} = 0$ , and  $\epsilon_{23} = \epsilon_{32} = 0$ ).

In terms of the Helmholtz free energy  $A$  the equation of state for the electrolyte version of the SAFT approach (SAFT-VRE) can be written in terms of separate contributions as

$$\frac{A}{NkT} = \frac{A^{\text{IDEAL}}}{NkT} + \frac{A^{\text{MONO}}}{NkT} + \frac{A^{\text{ASSOC}}}{NkT} + \frac{A^{\text{IONS}}}{NkT} \quad (1)$$

where  $N$  is the number of molecules,  $k$  the Boltzmann constant, and  $T$  the temperature. Here,  $A^{\text{IDEAL}}$  is the free energy of the ideal fluid,  $A^{\text{MONO}}$  represents the residual free energy of the monomers,  $A^{\text{ASSOC}}$  is the contribution due to association, and  $A^{\text{IONS}}$  is the residual free energy of the ion–ion interactions. We have not included the usual contribution due to chain formation as all the molecules considered are spherical. The fluid is assumed to be a mixture of water and ions in solution only; no undissociated salt molecules are present. Full details of the SAFT-VR approach have been presented elsewhere,<sup>47,48</sup>



here we briefly recap the general expressions for a multicomponent mixture and concentrate on the specific expressions of a ternary mixture of water (component 1) + cation (component 2) + anion (component 3); the expressions can then be readily extended to a solution containing several different ions.

**2.1. Ideal Contribution.** The free energy of the ideal mixture is given by<sup>55</sup>

$$\frac{A^{\text{IDEAL}}}{NkT} = \sum_{i=1}^n x_i \ln \rho_i \Lambda_i^3 - 1$$

$$= x_1 \ln \rho_1 \Lambda_1^3 + x_2 \ln \rho_2 \Lambda_2^3 + x_3 \ln \rho_3 \Lambda_3^3 - 1 \quad (2)$$

where  $\rho_i = N_i/V$  is the number density and  $\Lambda_i$  is the thermal de Broglie wavelength of species  $i$ .

**2.2. Monomer Contribution.** In the general case of a fluid with chain molecules the monomer free energy is written in terms of the number of spherical segments  $m_i$  building up a chain of component  $i$  as<sup>47,48</sup>

$$\frac{A^{\text{MONO}}}{NkT} = \left( \sum_{i=1}^n x_i m_i \right) \frac{A^{\text{M}}}{N_s kT}$$

$$= \left( \sum_{i=1}^n x_i m_i \right) a^{\text{M}} \quad (3)$$

where  $N_s$  is the total number of spherical segments. Since in our present work all species are spherical ( $m_i = 1$ ) the relation between the number of molecules and the number of spherical segments is trivial, i.e.,  $N = N_s$ . We can write directly

$$\frac{A^{\text{MONO}}}{NkT} = a^{\text{M}} \quad (4)$$

where  $a^{\text{M}}$  is obtained from the Barker and Henderson high-temperature expansion<sup>56,57</sup> as

$$a^{\text{M}} = a^{\text{HS}} + \beta a_1 + \beta^2 a_2 \quad (5)$$

$a^{\text{HS}}$  is the free energy for a mixture of hard spheres,  $\beta = 1/kT$ , and  $a_1$  and  $a_2$  are the first two terms of the perturbation expansion associated with an attractive energy  $-\epsilon_{ij}$ :  $a_1$  is the mean attractive energy and  $a_2$  describes the fluctuations in the energy of the fluid due to the attractive well.

The free energy for a mixture of hard-spheres of different sizes is obtained from the expression of Boublík<sup>58</sup> and Mansoori et al.<sup>59</sup>

$$a^{\text{HS}} = \frac{6}{\pi\rho} \left[ \left( \frac{\zeta_2^3}{\zeta_3^2} - \zeta_0 \right) \ln(1 - \zeta_3) + \frac{3\zeta_1\zeta_2}{1 - \zeta_3} + \frac{\zeta_2^3}{\zeta_3(1 - \zeta_3)^2} \right] \quad (6)$$

Note that the number density of the mixture  $\rho$  in our system is equivalent to the number density in terms of spherical segments  $\rho_s$  which is used in systems including chain molecules.<sup>47,48</sup> The reduced densities  $\zeta_c$  are then defined as

$$\zeta_c = \frac{\pi}{6} \rho \left[ \sum_{i=1}^n x_i (\sigma_{ii})^3 \right]$$

$$= \frac{\pi}{6} \rho (x_1 \sigma_{11}^3 + x_2 \sigma_{22}^3 + x_3 \sigma_{33}^3) \quad (7)$$

where  $\sigma_{ii}$  is the diameter and  $x_i$  the mole fraction of component  $i$ .

The mean attractive energy  $a_1$  is given by

$$a_1 = \sum_{i=1}^n \sum_{j=1}^n x_i x_j a_1^{ij} \quad (8)$$

where for a square-well potential with an energy  $-\epsilon_{ij}$  and range  $\lambda_{ij}$

$$a_1^{ij} = -\rho \alpha_{ij}^{\text{VDW}} g_{ij}^{\text{HS}}[\sigma_{ij}; \zeta_3^{\text{eff}}] \quad (9)$$

and  $\alpha_{ij}^{\text{VDW}}$  is the van der Waals attractive constant for the  $i$ - $j$  interaction,

$$\alpha_{ij}^{\text{VDW}} = 2\pi\epsilon_{ij}\sigma_{ij}^3(\lambda_{ij}^3 - 1)/3 \quad (10)$$

$\zeta_3^{\text{eff}}$  is an effective packing fraction, and  $g_{ij}^{\text{HS}}$  is the radial distribution function for a mixture of hard spheres evaluated at contact. In our present model only water–water and water–ion attractive square-well interactions are taken into account. The range and strength of these interactions are fitted to experimental data, while  $\sigma_{ij} = (\sigma_{ii} + \sigma_{jj})/2$ . The ion–ion square-well interactions are however set to zero ( $\epsilon_{22} = 0$ ,  $\epsilon_{33} = 0$ , and  $\epsilon_{23} = \epsilon_{32} = 0$ ). Hence, eq 8 includes only three terms in our mixture of water + cation + anion:

$$a_1 = x_1 a_1^{11} + 2x_1 x_2 a_1^{12} + 2x_1 x_3 a_1^{13} \quad (11)$$

Since in this work we are concerned with phase equilibria but will not deal with the critical region, we use mixing rule MX3b as defined in ref 48, so that

$$g_{ij}^{\text{HS}}[\sigma_{ij}; \zeta_3^{\text{eff}}] = \frac{1}{1 - \zeta_3^{\text{eff}}} + 3 \frac{D_{ij} \zeta_3^{\text{eff}}}{(1 - \zeta_3^{\text{eff}})^2} + 2 \frac{(D_{ij} \zeta_3^{\text{eff}})^2}{(1 - \zeta_3^{\text{eff}})^3} \quad (12)$$

where  $D_{ij}$  is

$$D_{ij} = \frac{\sigma_{ii} \sigma_{jj}}{\sigma_{ii} + \sigma_{jj}} \frac{\sum_{i=1}^n x_i \sigma_{ii}^2}{\sum_{i=1}^n x_i \sigma_{ii}^3} \quad (13)$$

and the effective packing fraction  $\zeta_3^{\text{eff}}$  is given by

$$\zeta_3^{\text{eff}}(\zeta_3, \lambda_{ij}) = c_1(\lambda_{ij})\zeta_3 + c_2(\lambda_{ij})\zeta_3^2 + c_3(\lambda_{ij})\zeta_3^3 \quad (14)$$

the coefficients  $c_1$ ,  $c_2$ , and  $c_3$  are given by the matrix

$$\begin{pmatrix} c_1 \\ c_2 \\ c_3 \end{pmatrix} = \begin{pmatrix} 2.258\,55 & -1.503\,49 & 0.249\,434 \\ -0.669\,270 & 1.400\,49 & -0.827\,739 \\ 10.157\,6 & -15.0427 & 5.308\,27 \end{pmatrix} \begin{pmatrix} 1 \\ \lambda_{ij} \\ \lambda_{ij}^2 \end{pmatrix} \quad (15)$$

The fluctuation term of the attractive energy for a mixture is given by

$$a_2 = \sum_{i=1}^n \sum_{j=1}^n x_i x_j a_2^{ij} \quad (16)$$

where we write each of the  $a_2^{ij}$  terms using the local compressibility approximation<sup>56</sup>

$$a_2^{ij} = \frac{1}{2} K^{\text{HS}} \epsilon_{ij} \rho \frac{\partial a_1^{ij}}{\partial \rho} \quad (17)$$

with  $K^{\text{HS}}$  the isothermal compressibility of a mixture of hard spheres; we use the Percus–Yevick equation<sup>60</sup>

$$K^{\text{HS}} = \frac{\zeta_0(1 - \zeta_3)^4}{\zeta_0(1 - \zeta_3)^2 + 6\zeta_1\zeta_2(1 - \zeta_3) + 9\zeta_2^3} \quad (18)$$

Substituting expression 9 for  $a_1^{\text{ij}}$  into expression 17 gives

$$a_2 = -\frac{1}{2}\rho K^{\text{HS}} \sum_{i=1}^n \sum_{j=1}^n x_i x_j \epsilon_{ij} \alpha_{ij}^{\text{VDW}} \times \left( g^{\text{HS}}[\sigma_{ij}; \zeta_3^{\text{eff}}] + \rho \frac{\partial g^{\text{HS}}[\sigma_{ij}; \zeta_3^{\text{eff}}]}{\partial \rho} \right) \quad (19)$$

Note that as indicated earlier  $\epsilon_{22} = 0$ ,  $\epsilon_{33} = 0$ , and  $\epsilon_{23} = \epsilon_{32} = 0$ , so that  $a_2$  in our mixture is given by

$$a_2 = x_1^2 a_2^{11} + 2x_1 x_2 a_2^{12} + 2x_1 x_3 a_2^{13} \quad (20)$$

**2.3. Association Contribution.** The contribution to the free energy due to the association of  $s_i$  sites on species  $i$  is obtained from the theory of Wertheim as<sup>61,62</sup>

$$\frac{A^{\text{ASSOC}}}{NkT} = \sum_{i=1}^n x_i \left[ \sum_{a=1}^{s_i} \left( \ln X_{a,i} - \frac{X_{a,i}}{2} \right) + \frac{s_i}{2} \right] \quad (21)$$

where the first sum is over the number of species  $i$  and the second over all  $s_i$  sites of type  $a$  on species  $i$ .  $X_{a,i}$  is the fraction of molecules of type  $i$  not bonded at site  $a$  and is obtained from the numerical solution of the mass action equations<sup>41,62</sup>

$$X_{a,i} = \frac{1}{1 + \sum_{j=1}^n \sum_{b=1}^{s_j} \rho x_j X_{b,j} \Delta_{a,b,i,j}} \quad (22)$$

The function  $\Delta_{a,b,i,j}$  characterizes the association between site  $a$  on molecule  $i$  and site  $b$  on molecule  $j$ ,

$$\Delta_{a,b,i,j} = K_{a,b,i,j} f_{a,b,i,j} g^{\text{M}}(\sigma_{ij}; \zeta_3) \quad (23)$$

$K_{a,b,i,j}$  is the volume available for bonding, a function of the position of the sites  $r_d$  and range  $r_c$  of the site–site interaction,  $f_{a,b,i,j}$  is the Mayer  $f$  function of the  $a - b$  interaction  $\phi_{a,b,i,j}$ ,  $f_{a,b,i,j} = \exp(-\phi_{a,b,i,j}/kT) - 1$ , and  $g^{\text{M}}(\sigma_{ij}; \zeta_3)$  is contact value of the radial distribution function of the reference unbonded square-well fluid. It is obtained from a temperature expansion as<sup>47,48</sup>

$$g^{\text{M}}(\sigma_{ij}; \zeta_3) = g_0^{\text{HS}}(\sigma_{ij}; \zeta_3) + \beta \epsilon_{ij} g_1(\sigma_{ij}; \zeta_3) \quad (24)$$

where  $g_0^{\text{HS}}(\sigma_{ij}; \zeta_3)$  is given by the Boublík<sup>58</sup> hard-sphere contact value

$$g_0^{\text{HS}}(\sigma_{ij}; \zeta_3) = \frac{1}{1 - \zeta_3} + 3 \frac{D_{ij} \zeta_3}{(1 - \zeta_3)^2} + 2 \frac{(D_{ij} \zeta_3)^2}{(1 - \zeta_3)^3} \quad (25)$$

and

$$g_1(\sigma_{ij}; \zeta_3) = g_0^{\text{HS}}[\sigma_{ij}; \zeta_3^{\text{eff}}] + (\lambda_{ij}^3 - 1) \frac{\partial g^{\text{HS}}[\sigma_{ij}; \zeta_3^{\text{eff}}]}{\partial \zeta_3^{\text{eff}}} \left( \frac{\lambda_{ij}}{3} \frac{\partial \zeta_3^{\text{eff}}}{\partial \lambda_{ij}} - \zeta_3 \frac{\partial \zeta_3^{\text{eff}}}{\partial \zeta_3} \right) \quad (26)$$

In our present model of electrolyte solutions only the water molecules are assumed to associate. From eq 21 the association

contribution to the free energy for a fluid with a four-site associating component is written as

$$\frac{A^{\text{ASSOC}}}{NkT} = x_1 \left[ 4 \left( \ln X_1 - \frac{X_1}{2} \right) + 2 \right] \quad (27)$$

since all four sites are equivalent in what concerns the fraction water molecules not bonded at a given site  $X_1$ , which is given by

$$X_1 = \frac{1}{1 + 2\rho x_1 X_1 \Delta_{11}} \quad (28)$$

The function  $\Delta_{11}$  is written in terms of the bonding volume available for the water sites  $K_{11}$ , the Mayer  $f$  function of the water–water site–site interaction  $F_{11} = \exp(\epsilon_{11}^{\text{HB}}/kT) - 1$ , and the radial distribution function of the water–water square-well segments in the mixture  $g^{\text{M}}(\sigma_{11}; \zeta_3)$  which is given by eqs 24–26:

$$\Delta_{11} = K_{11} F_{11} g^{\text{M}}(\sigma_{11}; \zeta_3) \quad (29)$$

At this level of approximation the extent of association depends only on the strength of the site–site interaction via  $F$  and on the range via  $K$ ; the precise details of the position and range of the sites are not important so long as they correspond to the same integrated volume.

It is clear that the SAFT treatment allows for straight forward extensions in which ion–ion association and saturable orientationally dependent solvation interactions between water and ions could also be included. As a first approximation we only allow the water molecules to associate and describe the water–ion interactions through the isotropic dispersive attractive energy described in the previous section. Further, as only aqueous solutions of very strong electrolytes (fully dissociated) over a moderate temperature range (up to 373 K) are examined, it is a reasonable approximation to disregard ion–ion association. In future we plan to study aqueous solutions of weak electrolytes as well as to extend our treatment toward the critical region of water; other association contributions will then be considered.

**2.4. Ionic Contribution.** In the RPM the anions and cations are represented as charged spheres of the same diameter interacting through a uniform medium of dielectric constant  $D$ ; the pair potential for the ion–ion interaction is given by<sup>15</sup>

$$u_{ij}(r) = \begin{cases} +\infty & \text{if } r < \tilde{\sigma} \\ (q_i q_j)/(Dr) & \text{if } r > \tilde{\sigma} \end{cases} \quad (30)$$

where  $i$  and  $j$  refer to the cation and anion, so that  $q_i = z_+ e$  and  $q_j = z_- e$ . The common hard-sphere diameter  $\tilde{\sigma}$  that represents the ions in the RPM is simply the average

$$\tilde{\sigma} = \sum_{j=2}^{\tilde{n}} \tilde{x}_j \sigma_{ij} \quad (31)$$

where the sum is over the number of ionic species  $\tilde{n}$ , i.e., does not include water (component 1). The fraction of ions  $\tilde{x}_j$  of a certain type within the total salt content can be calculated as

$$\begin{aligned} \tilde{x}_j &= \frac{N_j}{\sum_{j=2}^{\tilde{n}} N_j} \\ &= \frac{x_j}{\sum_{j=2}^{\tilde{n}} x_j} \end{aligned} \quad (32)$$

Waisman and Lebowitz<sup>19</sup> solved the Ornstein–Zernike equation for the RPM with the MSA closure:

$$\begin{aligned} g_{ij}(r) &= 0 \text{ if } r < \tilde{\sigma} \\ c_{ij}(r) &= -(q_i q_j)/(DkTr) \text{ if } r > \tilde{\sigma} \end{aligned} \quad (33)$$

where  $c_{ij}(r)$  is the direct correlation function. They derived an analytical solution which has found widespread use in the modeling of electrolyte solutions. In particular the excess free energy is given by<sup>15</sup>

$$\frac{A^{\text{IONS}}}{NkT} = -\frac{3x^2 + 6x + 2 - 2(1 + 2x)^{3/2}}{12\pi\rho\tilde{\sigma}^3} \quad (34)$$

where  $x = \kappa\tilde{\sigma}$ , and

$$\kappa^2 = \frac{4\pi}{DkT} \sum_{j=2}^{\tilde{n}} \rho_j q_j^2 \quad (35)$$

is the inverse Debye length. The radial distribution function at contact  $\tilde{\sigma}$  in the MSA treatment also takes a simple form; it is written as<sup>15</sup>

$$g_{ij}(\tilde{\sigma}) = g_{ij}^{\text{HS}}(\tilde{\sigma}) - \frac{q_i q_j}{DkT\tilde{\sigma}}(1 - \tau^2) \quad (36)$$

where

$$\tau = \frac{x^2 + x - x(1 + 2x)^{1/2}}{x^2} \quad (37)$$

The limit  $\tilde{\sigma} \rightarrow 0$  in eq 34 gives the DH free-energy expression:

$$\begin{aligned} \frac{A^{\text{IONS DH}}}{NkT} &= \lim_{\tilde{\sigma} \rightarrow 0} \frac{A^{\text{IONS}}}{NkT} \\ &= -\frac{\kappa^3}{12\pi\rho} \end{aligned} \quad (38)$$

In the DH theory the radial distribution function is given by

$$g_{ij}(r) = \exp\left[-\frac{q_i q_j}{DkT} \frac{e^{-\kappa r}}{r}\right] \quad (39)$$

although the expression is usually approximated by linearizing the external exponential so that

$$g_{ij}(r) = 1 - \frac{q_i q_j}{DkT} \frac{e^{-\kappa r}}{r} \quad (40)$$

As mentioned earlier, the DH model assumes point charges, which means that the function at contact must be evaluated for  $r \rightarrow 0$ . In our model, however, a hard-sphere repulsive contribution is also taken into account; in this case, a better approximation for the interionic radial distribution function at contact is<sup>63</sup>

$$g_{ij}(\tilde{\sigma}) = g_{ij}^{\text{HS}}(\tilde{\sigma}) \exp\left[\frac{q_i q_j}{DkT} \frac{e^{-\kappa\tilde{\sigma}}}{\tilde{\sigma}}\right] \quad (41)$$

Although not used in this work, eqs 36 and 41 become useful in a determination of the extent of ion–ion association within the SAFT approach (see eq 23).

In solutions of nonvolatile inorganic salts, such as the ones we study here, it is known that the vapor phase over the solution

is composed nearly exclusively of water. For example, the presence of NaCl in the vapor phase has been measured at temperatures above 380 °C (653 K), and was found to be of the order of 0.07%.<sup>64</sup> It is a reasonable approximation within the temperature range examined in this work ( $T < 373$  K) to restrict the ions to the liquid phase, so that the ionic term in eq 1 contributes only to the free energy of the liquid.

Once the expressions for the free energy of the fluid are known, the other thermodynamic properties can be obtained through standard relationships,<sup>55</sup> and the conditions for equilibria and critical properties are solved using a numerical method.<sup>65,66</sup> A more detailed discussion of the technique can be found in refs.<sup>55,56</sup> In a mixture it is necessary to write the parameters of the equation of state relative to one of the components, component 1 in our case:  $\sigma_{ij}^* = \sigma_{ij}/\sigma_{11}$ , and  $\alpha_{ij}^* = \alpha_{ij}/\alpha_{11}$ . The reduced site–site hydrogen-bond energy between the water molecules is given in terms of the integrated attractive energy of the square-well interaction,  $\alpha_{11}^{\text{VDW}}/b_{11}$  ( $b_{11} = \pi\sigma_{11}^3/6$ ), so that  $\epsilon_{11}^{\text{HB}*} = \epsilon_{11}^{\text{HB}} b_{11}/\alpha_{11}^{\text{VDW}}$ . The range and position of the sites are given in terms of the diameter of the sphere in which they are embedded ( $r_{\text{dl}}^* = r_{\text{dl}}/\sigma_{11}$  and  $r_{\text{cl}}^* = r_{\text{cl}}/\sigma_{11}$ ), and the bonding volume is then written as<sup>61</sup>

$$\begin{aligned} K_{11}^* &= \frac{K_{11}}{\sigma_{11}^3} = 4\pi[\ln(r_{\text{cl}}^* + 2r_{\text{dl}}^*)(6r_{\text{cl}}^{*3} + 18r_{\text{cl}}^{*2}r_{\text{dl}}^* - 24r_{\text{dl}}^{*3}) + \\ &\quad (r_{\text{cl}}^* + 2r_{\text{dl}}^* - 1)(22r_{\text{dl}}^{*2} - 5r_{\text{cl}}^*r_{\text{dl}}^* - 7r_{\text{dl}} - 8r_{\text{cl}}^{*2} + r_{\text{cl}}^* + 1)]/ \\ &\quad (72r_{\text{dl}}^{*2}) \end{aligned} \quad (42)$$

The temperature and pressure are also written as reduced dimensionless variables,  $T^* = kTb_{11}/\alpha_{11}^{\text{VDW}}$  and  $p^* = pb_{11}^2/\alpha_{11}^{\text{VDW}}$ .

### 3. Results and Discussion

We have studied the vapor pressures and densities of nine aqueous solutions of single strong electrolytes, and of a solution containing two salts. As mentioned earlier the salts are considered to be fully dissociated, and because the ions are very nonvolatile, they are restricted to the liquid phase. In order to be able to compare our calculations with experimental data the intermolecular potential parameters involved in the models need to be determined.

In the case of the water molecule the parameters are obtained from a best fit to experimental vapor pressures and saturated liquid densities from the triple point to the critical point<sup>67</sup> using a simplex method.<sup>65</sup> The optimized value for the hard-sphere diameter of the water molecule is  $\sigma_{11} = 3.036$  Å, the range of the square-well attractive interaction is  $\lambda_{11} = 1.8$ , and the energy  $\epsilon_{11}/k = 253.3$  K. The energy for the site–site interaction is  $\epsilon_{11}^{\text{HB}}/k = 1366$  K ( $\epsilon_{11}^{\text{HB}*} = 0.279$ ), with a bonding volume  $K_{11} = 1.028$  Å<sup>3</sup> (which corresponds to  $r_{\text{dl}}^* = 0.25$ , which is not optimized, and  $r_{\text{cl}}^* = 0.692$ ). A comparison of the experimental data with the calculations using this set of parameters is shown in Figure 1 and has also been presented in a recent publication.<sup>54</sup>

The determination of the parameters for the salt molecules cannot be carried out in an equivalent way to those of water since no experimental data of the vapor pressures or saturated liquid densities is available. Instead, we use experimental values where available. The experimental Pauling radii are used for each of the ions (see Table 1), while no ion–ion square-well interaction is included ( $\epsilon_{jj} = 0$  ( $j$  refers to the ions)). The cross parameters describing the square-well water–ion interaction,

**TABLE 1: Pauling Ionic Diameters and Optimized Water–Ion Interaction Parameters for Six Ions: Na<sup>+</sup>, K<sup>+</sup>, Li<sup>+</sup>, Cl<sup>−</sup>, Br<sup>−</sup>, I<sup>−</sup><sup>a</sup>**

	$\sigma_{ij}/\text{\AA}$	$\sigma_{1j}/\text{\AA}$	$(\epsilon_{1j}/k)/\text{K}$	$\lambda_{1j}$	$\alpha_{1j}^{\text{VDW}}$
Na <sup>+</sup>	1.90	2.468	2126	1.2	0.31
K <sup>+</sup>	2.66	2.848	94.60	1.2	0.31
Li <sup>+</sup>	1.36	2.198	782.8	1.2	0.53
Cl <sup>−</sup>	3.62	3.328	307.2	1.2	0.31
Br <sup>−</sup>	3.92	3.478	149.1	1.2	0.40
I <sup>−</sup>	4.40	3.718	152.6	1.2	0.50

<sup>a</sup>  $\sigma_{ij}$  is the ionic radius,  $\sigma_{1j}$  the unlike water–ion hard-sphere radius,  $\epsilon_{1j}$  the attractive square-well water–ion energy,  $\lambda_{1j}$  the potential range, and  $\alpha_{1j}^{\text{VDW}}$  the integrated attractive energy.

the range  $\lambda_{1j}$  and integrated attractive energy  $\alpha_{1j}^{\text{VDW}}$  (see eq 10), need to be determined from an examination of the mixture properties. The range  $\lambda_{1j}$  is set to 1.2 in all the solutions studied; a good description of the solution densities is obtained with this value of the unlike range parameter. The integrated energy is determined with the aid of the experimental vapor pressures of the solutions. An  $\alpha_{1j}^{\text{VDW}}$  is determined per ion regardless of the salt it may form part of. In this way, a small number of parameters allows for the study of a wide range of salts. In Table 1 the parameters describing the ion–water interaction of the six ions examined are presented. It is important to note that the depth of the square well for a given integrated energy is a function of the diameter of the segment (cf. eq 10) so that equal values of  $\alpha_{1j}^{\text{VDW}}$  may result in differing square-well energies  $\epsilon_{1j}$ .

Ideally, the dielectric constant takes a value of unity when the solvent is treated explicitly in a non-primitive model. The SAFT-VR approach, used in this work to model the water molecules,<sup>54</sup> includes part of the interactions that give rise to the bulk dielectric constant, but since this is done in an effective way via square-well and site–site potentials, a dielectric constant must be included to deal with the water–ion electrostatic interactions. Although a value smaller than that of the bulk may be expected since dipole–ion and ion–ion thermodynamics are included (at least in part), we take the experimental value at each temperature<sup>67</sup> as in this way there is one less parameter to adjust. This ad hoc approach has been shown to give very good agreement for the thermodynamic properties of the solutions<sup>33</sup> as compared to other models without these dipole–ion contributions.

As mentioned earlier, we use the expressions of the MSA to describe the contribution to the free energy due to the Coulombic interactions. In a future paper we will be examining more closely different expressions for the ionic contribution in the equation, but it is interesting to see here how using the DH expression (eq 38) in the SAFT-VRE equation still provides a very good agreement for the vapor pressures.

The experimental vapor pressures for three constant temperatures (up to 373 K)<sup>8</sup> and solution densities at 373 K<sup>8</sup> for an aqueous solution of NaCl are compared with the SAFT-VRE calculations in Figure 3. The mean spherical (solid curves) and the DH (dashed curves) approximations are presented. The parameters used for the water–ion interactions in the MSA are presented in Table 1. The DH calculations were done with an unlike range parameter  $\lambda_{1j} = 1.5$  which gives reasonable agreement for the density; as with the MSA treatment the integrated water–ion attractive energy is optimized by fitting to the experimental data of the mixture, giving  $\alpha_{1j}^{\text{VDW}} = 0.93$ , which corresponds to  $\epsilon_{12}/k = 892.2$  K for the water–Na<sup>+</sup> interaction, and  $\epsilon_{13}/k = 363.9$  K for water–Cl<sup>−</sup>. As can be seen in the figures, both the mean spherical and the DH approxima-

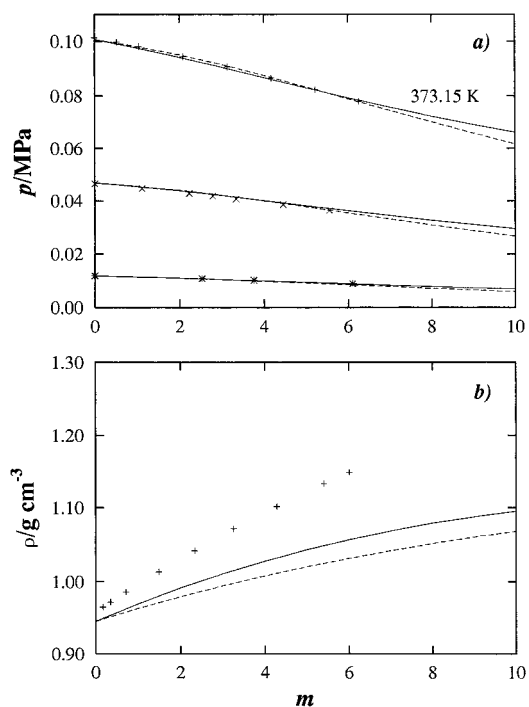


**Figure 3.** Experimental data of aqueous NaCl for (a) the vapor pressures at temperatures 373.15, 353.15, and 322.28 K, and (b) solution densities at 373.15 K compared with the SAFT-VRE calculations. The continuous curves correspond to the calculations using the mean spherical approximation for the ion–ion contribution and the dashed curves to the Debye–Hückel approximation. The symbols correspond to the experimental data.

tions provide an excellent agreement with the experimental pressures in the range of temperatures studied for salt concentrations up to 10m.

It is important to remark at this point that the DH approach is exact in the limit of infinite dilution, meaning that the model incorporates the right electrostatic contributions for the electrolyte solution. When the repulsive contribution due to the cores of the molecules in the solution are introduced together with the DH expression for the electrostatic contribution, an accurate and simple equation is obtained.<sup>30</sup> As expected, the densities of the solutions are better described by the MSA treatment which includes higher density correlations; when tested against computer simulation it is clearly superior to the DH approach in what concerns to the structure of the fluid.<sup>13</sup> All of the calculated results that follow in this work have been obtained using the expressions of the MSA for the ionic energy contribution.

Experimental vapor pressures<sup>8</sup> and solution densities<sup>8</sup> for concentrations up to 10m are compared with the SAFT-VRE calculations for three aqueous solutions of sodium halides (NaCl, NaBr, and NaI) in Figure 4: the vapor pressures of each of the solutions at temperatures from 273 to 373 K are shown; the densities for the three solutions at 298 K for NaCl and NaBr and at 288 K for NaI are also presented. Analogous figures for three aqueous solutions of potassium halides (KCl, KBr, and KI) are presented in Figure 5. Experimental vapor pressures<sup>8</sup> are again compared with theoretical calculations for temperatures from 273 to 373 K; the experimental solution densities<sup>8</sup> are compared with the calculations at temperatures of 313 K for KCl, 288 K for KBr, and 293 K for KI. As can be seen from the figures, very good agreement with the experimental data is obtained. In Figure 6 the experimental vapor pressures<sup>8</sup> for aqueous LiCl from 273 to 373 K up to 10m are compared with the SAFT-VRE calculations using the parameters in Table 1



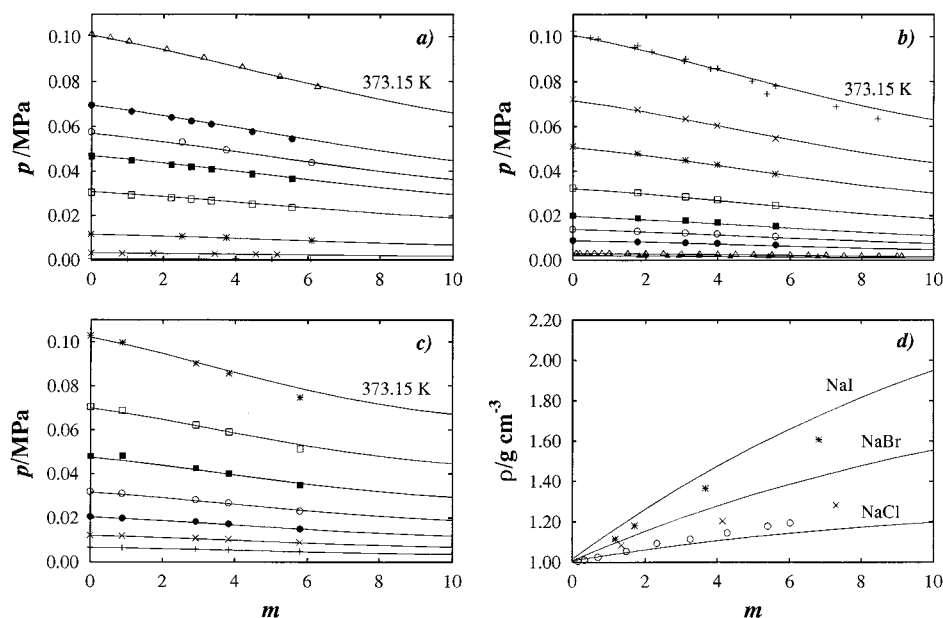


**Figure 4.** Experimental vapor pressures of (a) aqueous NaCl at temperatures 373.15, 363.15, 358.01, 353.15, 343.15, 322.28, 298.74, and 273.15 K; (b) aqueous NaBr at temperatures 373.15, 363.91, 355.04, 344.11, 333.23, 325.68, 316.84, 298.15, and 291.15 K; (c) aqueous NaI at temperatures 373.57, 363.31, 353.48, 343.77, 333.97, 323.03, and 311.44 K; and (d) solution densities for NaCl at 298.15 K, NaBr at 298.15 K, and NaI at 288.15 K. The experimental data are represented with symbols and the calculations with curves.

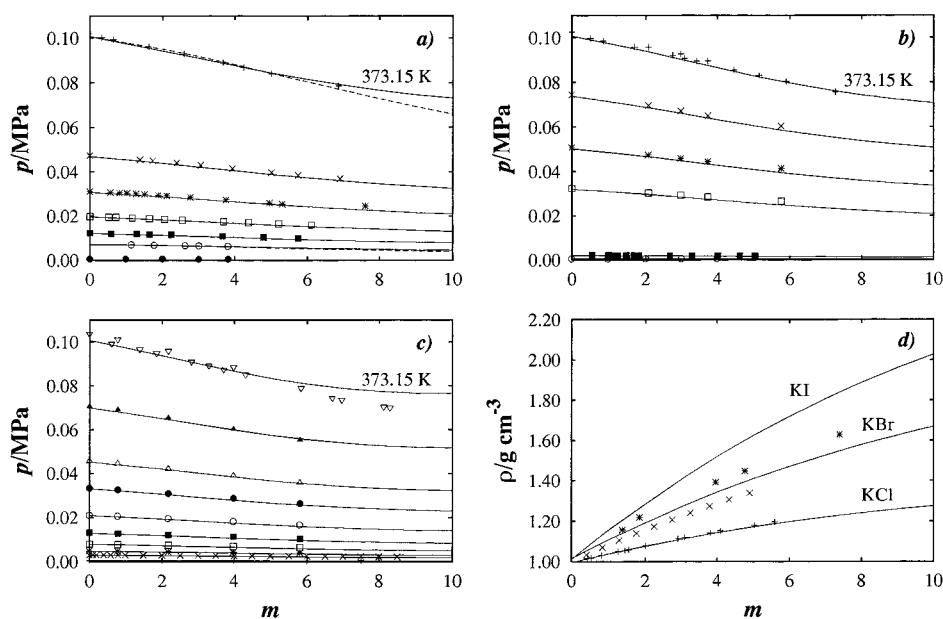


**Figure 5.** Experimental vapor pressures of (a) aqueous KCl at temperatures 373.15, 353.15, 343.15, 333.15, 323.15, 313.15, and 273.15 K; (b) aqueous KBr at temperatures 373.15, 364.76, 354.86, 344.03, 291.15, and 273.15 K; (c) aqueous KI at temperatures 373.15, 363.33, 352.30, 344.79, 334.47, 324.31, 314.94, 305.85, 298.15, and 273.15 K; and (d) solution densities for aqueous KCl at 313.15 K, KBr at 288.15 K, and KI at 293.15 K. The experimental data are represented with symbols and the calculations with curves.

for  $\text{Li}^+$  and  $\text{Cl}^-$ . The theory provides a very good description of the experimental measurements for the entire temperature range studied. The density of the solution at 298 K is also examined. Although the theory predicts an increase in density which is less marked than that of the experimental data, the maximum error at 10m is less than 5%. The vapor pressures of LiBr and LiI are studied at temperatures from 303 to 343 K<sup>68</sup> up to 10m (see Figure 7) using the parameters for the ions presented in Table 1. Excellent agreement with the experimental data is again found for both mixtures.

One of the main advantages of our approach is that it can be readily extended to solutions of mixed salts without the need for further parameter optimization. Because the potential parameters are determined in terms of the ions, they are

transferable to different salts containing a given ion. In this way the parameters presented in Table 1 for six ions allow the study of a wide range of single and multiple-salt solutions. The average diameter for all ions in the RPM ionic contribution is obtained using eq 31. To demonstrate the predictive power of the SAFT-VRE approach we have calculated the vapor pressures of a combined solution of LiBr and LiI<sup>69</sup> at temperatures from 313–343 K for total concentrations up to 10m. The salts are present in the solution in a ratio 4:1 of LiBr to LiI. As can be seen in Figure 7, excellent agreement with the experimental data is also found for this multicomponent mixture without any readjustment of the parameters.

It is encouraging to consider that our very simple model reproduces many of the features of the experimental solutions.

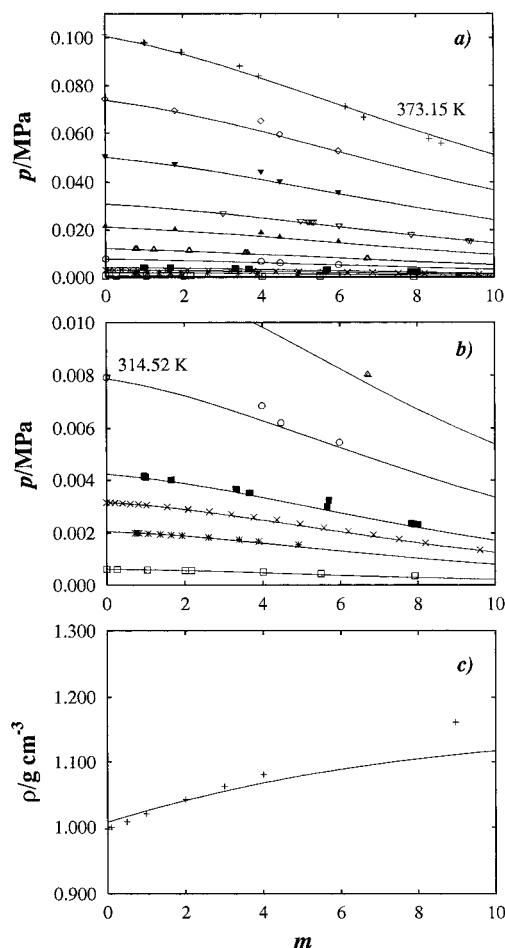


**Figure 6.** Experimental vapor pressures at (a) 373.15, 364.73, 354.80, 343.15, 334.81, and 323.15 K; and (b) at 314.52, 303.15, 298.15, 291.15, and 273.15 K; and (c) solution densities at 298.15 K compared with SAFT-VRE calculations for an aqueous solution of LiCl. The symbols represent the experimental data and the curves the SAFT-VRE calculations. The vapor pressures in the low temperature region below 314.52 K (circles) are better seen in part b.

Recall that only two parameters need to be fitted to mixture properties (the range and depth of the ion–water interaction), while the other parameters related to the ions (the ion diameter and the dielectric constant) take their experimental values and are not fitted. The vapor pressures calculated with the SAFT-VRE equation are in excellent agreement with the experimental data for all the salts studied. The densities are also well reproduced although in general the SAFT-VRE calculations predict a more marked increase in density with increasing salt concentration. It should be noted, however that the error is always less than 5%, and that the ion sizes have been obtained from experimental Pauling diameters; the ionic radii are more commonly fitted to experimental mixture data.<sup>30,31,33</sup>

This is the first of a number of studies in which we aim to model aqueous electrolyte solutions taking advantage of the success of the SAFT-VR approach in describing complex systems. Using a good model for water<sup>54</sup> we have shown how even a very crude approach for the ion–ion interaction, including solvent–ion interactions, provides a good agreement with experiment for the vapor–liquid equilibrium of the electrolyte solutions. Our present treatment leaves room for improvement. In terms of the temperature range considered we aim at comparing our calculations with the extensive data of Bischoff and Pitzer<sup>9</sup> in the critical region. Additionally, weak electrolytes and associated electrolytes can easily be included

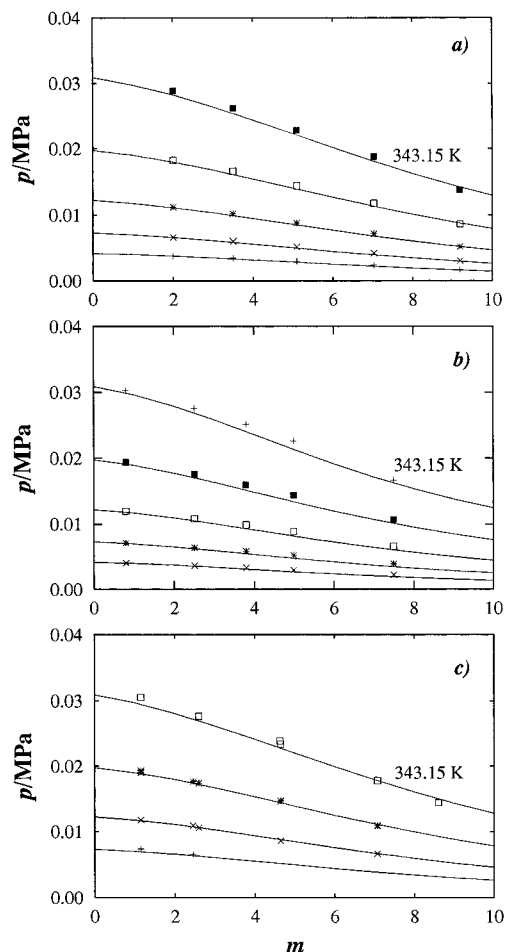


**Figure 7.** Experimental vapor pressures for aqueous solutions of (a) LiBr, and (b) LiI at temperatures of 343.15, 333.15, 323.15, 313.15, and 303.15 K compared with SAFT-VRE calculations. The experimental vapor pressures for an aqueous solution of LiBr and LiI in a ratio 4:1 (LiBr:LiI) at temperatures of 343.15, 333.15, 323.15, and 313.15 K are compared with SAFT-VRE calculations in part c. The symbols represent the experimental data and the curves the SAFT-VRE calculations.

in the SAFT formalism; for example, the detailed three-step mechanisms for ion pairing proposed by Chialvo et al.<sup>4</sup> can be incorporated into the SAFT-VRE approach. Finally, more accurate approximations than the RPM can be used for the evaluation of the free energy due to the ion–ion interaction.

**Acknowledgment.** A.G. and A.G.V. thank ICI Chemicals and Polymers Ltd. for funding Research Fellowships. We also acknowledge support from the Royal Society, and the Computational and ROPA Initiatives of the EPSRC for computer hardware on which the calculations were performed.

## References and Notes

- (1) Robinson, R. A.; Stokes, R. H. *Electrolyte Solutions*, 2nd ed.; Butterworths: London, 1965.
- (2) Bjerrum, N. K. *Vidensk. Selsk.* **1926**, 7, No. 9.
- (3) Pitzer, K. S. *J. Chem. Thermodyn.* **1993**, 25, 7.
- (4) Chialvo, A. A.; Cummings, P. T.; Cochran, H. D.; Simonson, J. M.; Mesmer, R. E. *J. Chem. Phys.* **1995**, 103, 9379.
- (5) Palaban, R. T.; Pitzer, K. S. *J. Chem. Eng. Data* **1988**, 33, 354.
- (6) Cummings, P. T.; Chialvo, A. A. *J. Phys. Condens. Matter* **1996**, 8, 9281.
- (7) Horvath, A. L. *Handbook of Aqueous Electrolyte Solutions*; Ellis Horwood Ltd.: Chichester, 1985.
- (8) Timmermans, J. *The Physicochemical Constants of Binary Systems in Concentrated Solutions*; Interscience: New York, 1960; Vol. 3.
- (9) Bischoff, J. L.; Pitzer, K. S. *Am. J. Sci.* **1989**, 289, 217.

- (10) Bischoff, J. L. *Am. J. Sci.* **1991**, 291, 309.
- (11) Arrhenius, S. A. Z. *Phys. Chem.* **1887**, 1, 285.
- (12) Debye, P.; Hückel, E. Z. *Phys.* **1923**, 24, 195; Z. *Phys.* **1923**, 24, 305.
- (13) Outhwaite, C. W. *Spec. Period. Rep.* **1975**, 2, 188.
- (14) Guggenheim, E. A. *Applications of Statistical Mechanics*; Clarendon Press: Oxford, 1966.
- (15) Lee, L. L. *Molecular Thermodynamics of Non-Ideal Fluids*; Butterworths: Boston, 1988.
- (16) Pitzer, K. S. *J. Phys. Chem.* **1973**, 77, 268.
- (17) Pitzer, K. S. *J. Sol. Chem.* **1975**, 4, 249.
- (18) Pitzer, K. S. *Acc. Chem. Res.* **1977**, 10, 371.
- (19) Waisman, E.; Lebowitz, J. L. *J. Chem. Phys.* **1970**, 52, 4307.
- (20) Blum, L. *Mol. Phys.* **1975**, 30, 1529.
- (21) Baxter, R. J. *J. Chem. Phys.* **1970**, 52, 4559.
- (22) Adelman, S. A.; Deutch, J. M. *J. Chem. Phys.* **1974**, 60, 3935.
- (23) Loehe, J. R.; Donohue, M. D. *AIChE J.* **1997**, 43, 180.
- (24) Shiah, I. M.; Tseng, H. C. *Fluid Phase Equilibria* **1994**, 90, 75.
- (25) Gering, K. L.; Lee, L. L.; Landis, L. H. *Fluid Phase Equilib.* **1989**, 48, 111.
- (26) Planche, H.; Renon, H. *J. Phys. Chem.* **1981**, 85, 3924.
- (27) Copeman, T. W.; Stein, F. P. *Fluid Phase Equilib.* **1987**, 35, 165.
- (28) Stell, G.; Lebowitz, J. L. *J. Chem. Phys.* **1968**, 49, 3706.
- (29) Henderson, D.; Blum, L.; Tani, A. American Chemical Society Symposium Series 300; American Chemical Society: Washington, 1985.
- (30) Chan, K. Y. *J. Phys. Chem.* **1990**, 94, 8472.
- (31) Chan, K. Y. *J. Phys. Chem.* **1991**, 95, 7465.
- (32) Carnahan, N. F.; Starling, K. E. *J. Chem. Phys.* **1969**, 51, 635.
- (33) Jin, G.; Donohue, M. D. *Ind. Eng. Chem. Res.* **1988**, 27, 1073.
- (34) Jin, G.; Donohue, M. D. *Ind. Eng. Chem. Res.* **1988**, 27, 1737.
- (35) Jin, G.; Donohue, M. D. *Ind. Eng. Chem. Res.* **1991**, 30, 240.
- (36) Wertheim, M. S. *J. Stat. Phys.* **1984**, 35, 19; *J. Stat. Phys.* **1984**, 35, 35.
- (37) Wertheim, M. S. *J. Stat. Phys.* **1986**, 42, 459; *J. Stat. Phys.* **1986**, 42, 477.
- (38) Wertheim, M. S. *J. Chem. Phys.* **1986**, 85, 2929.
- (39) Wertheim, M. S. *J. Chem. Phys.* **1987**, 87, 7323.
- (40) Chapman, W. G.; Gubbins, K. E.; Jackson, G.; Radosz, M. *Fluid Phase Equilib.* **1989**, 52, 31.
- (41) Chapman, W. G.; Gubbins, K. E.; Jackson, G.; Radosz, M. *Ind. Eng. Chem. Res.* **1990**, 29, 1709.
- (42) Huang, S. H.; Radosz, M. *Ind. Eng. Chem. Res.* **1990**, 29, 2284.
- (43) Huang, S. H.; Radosz, M. *Ind. Eng. Chem. Res.* **1991**, 30, 1994.
- (44) Galindo, A.; Whitehead, P. J.; Jackson, G.; Burgess, A. N. *J. Phys. Chem.* **1996**, 100, 6781.
- (45) García-Lisbona, M. N.; Galindo, A.; Jackson, J.; Burgess, A. N. *Mol. Phys.* **1998**, 93, 57.
- (46) García-Lisbona, M. N.; Galindo, A.; Jackson, G.; Burgess, A. N. *J. Am. Chem. Soc.* **1998**, 120, 4191.
- (47) Gil-Villegas, A.; Galindo, A.; Whitehead, P. J.; Mills, S. J.; Jackson, G.; Burgess, A. N. *J. Chem. Phys.* **1997**, 106, 4168.
- (48) Galindo, A.; Davies, L. A.; Gil-Villegas, A.; Jackson, G. *Mol. Phys.* **1998**, 93, 241.
- (49) Davies, L. A.; Gil-Villegas, A.; Jackson, G. *Int. J. Thermophys.* **1998**, 19, 675.
- (50) McCabe, C.; Gil-Villegas, A.; Jackson, G. *J. Phys. Chem. B*, **1998**, 102, 4183.
- (51) Galindo, A.; Gil-Villegas, A.; Whitehead, P. J.; Jackson, G.; Burgess, A. N. *J. Phys. Chem. B* **1998**, 102, 7632.
- (52) McCabe, C.; Galindo, A.; Gil-Villegas, A.; Jackson, G. *J. Phys. Chem. B* **1998**, 102, 8060.
- (53) McCabe, C.; Galindo, A.; Gil-Villegas, A.; Jackson, G. *Int. J. Thermophys.* **1998**, 19, 1511.
- (54) Grice, S. J.; Galindo, A.; Jackson, G.; Burgess, A. N. *Phys. Chem. Chem. Phys.* **1999**. Submitted for publication.
- (55) Rowlinson, J. S.; Swinton, F. L. *Liquids and Liquid Mixtures*, 3rd ed.; Butterworths: London, 1982.
- (56) Barker, J. A.; Henderson, D. *J. Chem. Phys.* **1967**, 47, 2856; *J. Chem. Phys.* **1967**, 47, 4714.
- (57) Barker, J. A.; Henderson, D. *Rev. Mod. Phys.* **1976**, 48, 587.
- (58) Boublik, T. *J. Chem. Phys.* **1970**, 53, 471.
- (59) Mansoori, G. A.; Carnahan, N. F.; Starling, K. E.; Leland, T. W. *J. Chem. Phys.* **1971**, 54, 1523.
- (60) Reed, T. M.; Gubbins, K. E. *Appl. Stat. Mech.*; McGraw Hill: New York, 1973.
- (61) Jackson, G.; Chapman, W. G.; Gubbins, K. E. *Mol. Phys.* **1988**, 65, 1.
- (62) Chapman, W. G.; Jackson, G.; Gubbins, K. E. *Mol. Phys.* **1988**, 65, 1057.
- (63) McQuarrie, D. A. *Statistical Thermodynamics*; Harper's Chemistry Series, Harper and Row: New York, 1973.
- (64) Parisod, C. J.; Plattner, E. *J. Chem. Eng. Data*, **1981**, 26, 16.
- (65) Press, W. H.; Teukolsky, S. A.; Vetterling, W. T.; Flannery, B. P. *Numerical Recipes in Fortran*, 2nd ed; Cambridge University Press: Cambridge, MA, 1986.
- (66) Scott, R. L.; van Konynenburg, P. H. *Discuss. Faraday Soc.* **1970**, 49, 87. van Konynenburg, P. H.; Scott, R. L. *Philos. Trans. R. Soc. London Ser. A* **1980**, 298, 495.
- (67) *Handbook of Chemistry and Physics*; CRC Press: Boca Raton, 1980.
- (68) Patil, K. R.; Tripathi, A. D.; Pathak, G.; Katti, S. S. *J. Chem. Eng. Data* **1990**, 35, 166.
- (69) Iyoki, S.; Iwasaki, S.; Uemura, T. *J. Chem. Eng. Data* **1990**, 35, 429.